

1 The VOL-CALPUFF Model for Atmospheric Ash
2 Dispersal: I. Approach and Physical Formulation

S. Barsotti, A. Neri

3 Istituto Nazionale di Geofisica e Vulcanologia - Sezione di Pisa, Pisa, Italy

J. S. Scire

4 TRC Companies, Inc., Atmospheric Studies Group, Lowell, Massachusetts,

5 USA

S. Barsotti, INGV - Sezione di Pisa - Via Della Faggiola 32, 56126 Pisa, Italy

A. Neri, INGV - Sezione di Pisa - Via Della Faggiola 32, 56126 Pisa, Italy

J. S. Scire, Atmospheric Studies Group -TRC Companies, Inc., Lowell, Massachusetts, USA

6 **Abstract.** We present a new modeling tool, named VOL-CALPUFF able
7 to simulate the transient and three-dimensional transport and deposition of
8 volcanic ash under the action of realistic meteorological and volcanological
9 conditions throughout eruption duration. The new model derives from the
10 CALPUFF System, a software program widely-used in environmental ap-
11 plications of pollutant dispersion, that describes the dispersal process both
12 in the proximal and distal regions and also in presence of complex orogra-
13 phy. The main novel feature of the model is its capability of coupling a Eulerian
14 description of plume rise with a Lagrangian representation of ash dispersal
15 described as a series of diffusing packets of particles or puffs. The model is
16 also able to describe the multiparticle nature of the mixture as well as the
17 tilting effects of the plume due to wind action. The dispersal dynamics and
18 ash deposition are described by using refined orography-corrected meteorolo-
19 gical data with a spatial resolution up to 1 km or less and a temporal step
20 of 1 hour. The modeling approach also keeps the execution time to a few minutes
21 on common PCs, thus making VOL-CALPUFF a possible tool for the pro-
22 duction of ash dispersal forecasts for hazard assessment. Besides the model
23 formulation, the paper presents the type of outcomes produced by VOL-CALPUFF,
24 shows the effect of main model parameters on results, and also anticipates
25 the fundamental control of atmospheric conditions on the ash dispersal processes.
26 In the companion paper (*Barsotti and Neri* [2007], this issue) a first thor-
27 ough application of VOL-CALPUFF to the simulation of a weak plume at

²⁸ Mount Etna (Italy) is presented with the specific aim of comparing model
²⁹ predictions with independent observations.

1. Introduction and Background

30 Amongst the processes associated with an explosive eruption, ash dispersal is proba-
31 bly the phenomenon occurring on the widest range of spatial and temporal scales. Ash
32 particles can have mostly local and regional effects lasting for a few days, if the volcanic
33 column is contained within the troposphere. On the other hand, larger plumes reaching
34 the stratosphere can have a global impact and drive climatic changes for several years.
35 Ash dispersal and fallout can also represent a major hazard for populations near volcanic
36 centers, producing a serious risk for human and animal health and causing damage to
37 crops, ground infrastructures, and aviation traffic (*Sparks et al.* [1997]; *Sigurdsson et al.*
38 [2000]; *Martì and Ernst* [2005]). Due to such a frequent and wide impact of ash fallout the
39 scientific community has produced, for many years, numerical models aimed at describ-
40 ing the rising phase and movements of volcanic particles in the atmosphere. Modeling
41 volcanic ash dispersal is indeed a complex task. It needs detailed information on the
42 system initial and boundary conditions as the volcanic source and temporal and spatial
43 meteorological variations, as well as on the physics that govern the entire phenomenon.
44 Historically, physical models can be roughly divided into two categories: 1) those aimed
45 at describing the dynamics of the volcanic column, and 2) those focused on the description
46 of pyroclast dispersal in the atmosphere and at the ground. In the following paragraphs
47 the main physical models, developed to date, will be briefly recalled together with their
48 main features.

49 **Volcanic column** Regarding this first category, early models adopted a pseudofluid ap-
50 proach in which solid particles and gases are assumed to be in thermal and mechanical

51 equilibrium thus forming a mixture characterized by a bulk density (*Wilson* [1976]; *Wilson*
52 *and Walker* [1987]; *Sparks et al.* [1997]). The main features of the rising plume phase were
53 described by solving the conservation equations of mass and momentum for the homoge-
54 neous mixture and assuming a steady time-averaged 1-D axisymmetric column. Later on,
55 the equation sets of these so-called “plume-theory” models were integrated by adding the
56 energy conservation equation in different forms (*Woods* [1988]; *Glaze and Baloga* [1996]).
57 Further developments concerned the modeling of thermal disequilibrium (*Woods and Bur-*
58 *sik* [1991]), particle fallout from the column (*Woods and Bursik* [1991]; *Ernst et al.* [1996]),
59 and umbrella cloud (*Bursik et al.* [1992b]; *Bonadonna et al.* [1998]) and particle recycling
60 into the eruption column (*Ernst et al.* [1996]; *Veitch and Woods* [2002]; *Veitch and Woods*
61 [2004]; *Textor et al.* [2004]). Crosswind influence on plume tilting has also been addressed
62 based on experimental and theoretical work on turbulent buoyant plumes in cross flow
63 (*Hoult and Weil* [1972]; *Wright* [1984]; *Ernst et al.* [1994]; *Bursik* [2001]). These types of
64 models were also used to obtain simple correlations to estimate column height (*Carey and*
65 *Sparks* [1986]; *Bursik et al.* [1992a]; *Bonadonna et al.* [1998]). The evaluation of column
66 height is indeed crucial for quantifying the area affected by ash fallout. These correlations
67 link column height with the excess thermal energy associated with the column (*Morton*
68 *et al.* [1956]; *Morton* [1959]) or directly with the mass flow rate (*Sparks* [1986]; *Sparks*
69 *et al.* [1997]). Similar dimensional arguments are used to estimate column height in a
70 windy environment (*Wright* [1984]). The dynamics of buoyant volcanic columns have
71 also been recently investigated by adopting transient, multidimensional, and multiphase
72 flow models able to describe new features of the phenomenon. For instance, the ATHAM
73 code (*Oberhuber et al.* [1998]; *Herzog et al.* [1998]; *Graf et al.* [1999]; *Textor et al.* [2004];

74 *Textor et al.* [2006a]; *Textor et al.* [2006b]) is a fully 3D non-hydrostatic limited area
75 circulation model able to describe the eruption column behavior, including accurate cloud
76 physics and microphysical processes, on spatial scales of a few hundred kilometers and
77 up to few hours of eruption time. Similarly, *Dartevelle et al.* [2004] recently analyzed the
78 2D transient behavior of buoyant volcanic clouds of different scales by using a two-phase
79 mixture description. The influence of the third dimension and turbulence closure has been
80 discussed by *Suzuki et al.* [2005] by using a pseudogas approximation of the multiphase
81 mixture.

82 **Pyroclastic dispersal and deposition** With respect to this second category of models,
83 first attempts were by *Suzuki* [1983], *Armienti et al.* [1988], *Macedonio et al.* [1988], *Mace-*
84 *donio et al.* [1990] and, more recently, by *Macedonio et al.* [2005] and *Costa et al.* [2006],
85 who adopted advection-diffusion equations and solved them in 2D and 3D domains. Other
86 studies based on this approach discuss the effect of various parameterizations of the source
87 and the production of probabilistic hazard maps (*Bonadonna et al.* [2002]; *Bonadonna*
88 *et al.* [2005]; *Pfeiffer et al.* [2005]). In these models the volcanic column is parameterized
89 by an empirical source function and particles diffuse under the action of constant winds.
90 An alternative approach, mostly used to reproduce the deposit features, assumes the wind-
91 advected volcanic material to be spreading radially as an intrusive gravity current above
92 the level of neutral buoyancy (*Sparks et al.* [1991]; *Bursik et al.* [1992b]; *Bonadonna et al.*
93 [1998]). Models based on alternative approaches have also been developed by different
94 groups. The PUFF model (*Searcy et al.* [1998]) describes the movements of a collection of
95 discrete ash particles representing a sample of the eruption cloud by using a Lagrangian
96 scheme and treating the source as a virtual pre-assigned vertical distribution of mass.

97 Similarly, the HYSPLIT code (*Draxler and Taylor* [1982]; *Draxler and Hess* [1998]) de-
98 scribes, by means of a Lagrangian approach, the evolution of puffs (containing material
99 particles with diameters up to 30 μm) without taking account of buoyancy effects. Other
100 codes are in use at the Volcanic Ash Advisory Centers (VAACs). CANERM (*Simpson*
101 *et al.* [2002]) (operative at the Canadian Meteorological Center), is a 3D Eulerian model
102 used for medium- and long-range transport which assumes a virtual source described by
103 a vertical mass distribution. Similarly, MEDIA (*Piedelievre et al.* [1990]) (operative at
104 Toulouse Meteo France), is a Eulerian atmospheric transport/diffusion model focused on
105 long-range dispersal of particles ejected from a source at a given altitude. NAME (*Watkin*
106 *et al.* [2004]) (operative at the UK Met Office), is a Lagrangian particle model that can
107 be applied on either regional or global scales and is able to consider areal as well as point-
108 like sources. Finally, VAFTAD (*Heffter and Stunder* [1993]) (developed by NOAA ARL
109 and in use at the Washington and Anchorage VAACs), is a 3D time-dependent Eulerian
110 model which needs the maximum height reached by the volcanic column to model the
111 input source. Currently all the above models are of limited value for volcanic ash disper-
112 sal forecasting, despite being used at VAACs, in that they all lack a source-term matrix
113 derived from an understanding of basic eruption physics (GGJ. Ernst, pers. communica-
114 tion). This realization is one of the key motivations for developing the present work.

115

2. Aim of the Work

116 From the above summary it is clear that the dynamics of the rising volcanic plume and of
117 the dispersal and depositional processes have been mostly treated separately despite their
118 being part of the same phenomenon and being strictly inter-related. Moreover, volcanic

119 plume models typically cannot be applied under realistic meteorological conditions and,
120 similarly, dispersal models do not account for realistic source conditions as they adopt
121 what may appear as subjective parameterization of the source. Finally, most of the
122 dispersal models in use at research and operative centers are relevant only to medium-
123 and long-distance areas, whereas the importance of forecasting the ash dispersal also in
124 proximal regions is crucial for nearby inhabited areas and aviation routes. In this case
125 a treatment of meteorological datasets able to include effects on wind fields due to the
126 presence of complex orography is also necessary. The aim of this work is to present a
127 new modeling system, named VOL-CALPUFF, able to simulate the transient and three-
128 dimensional injection, transport and deposition of volcanic ash under the action of realistic
129 and unperturbed meteorological and volcanological conditions. The main novel feature
130 of the model is its capability of coupling a Eulerian plume rise model with a Lagrangian
131 representation of ash dispersal described as a series of diffusing packets of particles or
132 “puffs”. Like several other codes used in volcanological applications, VOL-CALPUFF has
133 its origin in an air quality modeling code named CALPUFF designed for the transport of
134 pollutants at local and long-distance scales (*Nguyen et al.* [1997]; *Scire et al.* [2000]). The
135 VOL-CALPUFF code differs from the original CALPUFF code in several aspects fully
136 described in this paper, which makes it suitable for volcanological applications. The main
137 differences include the implementation of a multiparticle plume model, the possibility of
138 treating particles larger than a few microns, the consideration of puff dispersal well above
139 the atmospheric boundary layer, and the consideration of various settling velocity laws as
140 a function of particle size and shape. It is also worth noting that the VOL-CALPUFF code
141 can describe the whole dispersal dynamics and deposition by using very refined orography-

142 corrected meteorological data - with a final resolution up to 1 km or less - while keeping
143 the execution time in the order of minutes on common PCs. All these features also make
144 VOL-CALPUFF a promising tool for the production of ash dispersal forecasts for hazard
145 assessment. In the following sections an overview of the CALPUFF System, the main
146 features of the new VOL-CALPUFF code, and some sensitivity tests for weak plumes,
147 will be presented. The companion paper (*Barsotti and Neri* [2007], this issue) will present
148 a first complete application of the new code to a weak plume of Mt. Etna.

3. An Overview of the CALPUFF System

149 With the term “CALPUFF System” we mean the whole numerical procedure that from
150 meteorological and geophysical input data computes hourly the concentration of released
151 material, gaseous or particulate, in the atmosphere and at the ground. The CALPUFF
152 system was developed by Earth Tech Inc. (now TRC Companies, Inc.) in the 1990s
153 and it is freely available on line at the website <http://www.src.com/calpuff/calpuff1.htm>.
154 CALPUFF is a quite complex model composed of a great number of sub-processors linked
155 to each other by an input-output data flow. It has a modular structure, so that, depending
156 on the available input data and type of information required, the model elaboration can
157 follow different patterns. Fig. 1 shows a simplified basic configuration of the system such
158 as the one we have used in our study. The procedure starts with the elaboration of the
159 geophysical information, such as terrain elevation and land-use data, once the choice of
160 the computational domain under investigation is made. In parallel with the elaboration
161 of the geophysical information, processing of the meteorological data occurs to provide
162 CALMET (see hereafter) with the necessary input data. The meteorological processor
163 CALMET is a diagnostic code; this means that it computes the values of meteorological

164 variables on a finer grid without solving the time-dependent equation of motion. CALMET
165 works in two steps that refine and correct an initial guess field typically provided by a
166 prognostic code (e.g. MM5, ETA). In the first step the initial data are interpolated on a
167 grid usually much finer than that used in mesoscale models, and the local orography effects
168 are accounted for (*Scire et al.* [1990]; *Scire and Robe* [1997]). In the second step, surface
169 or upper air data, when available, are considered to correct the computed wind field
170 through an objective analysis that assigns appropriate weight to each data. The output
171 provided by CALMET contains the 3D fields (such as wind and temperature) and the 2D
172 field of micro-meteorological variables (like friction velocity, Obukhov length, atmospheric
173 boundary layer height and Pasquill-Gifford-Turner stability classes). All these variables
174 are computed with the temporal resolution required by the dispersal model and on a
175 grid in a terrain-following coordinate system with a vertical and horizontal user-defined
176 resolution. This file, together with that containing the data related to the volcanic source,
177 is fed as input to the system's core, i.e. the CALPUFF dispersal model.

178 The CALPUFF code describes atmospheric ascent and dispersion of a gaseous mixture
179 under the action of advective, turbulent wind fields. The rising plume phase is computed
180 in a Eulerian way by solving the plume theory equation, whereas dispersal is described
181 in a Lagrangian framework. In particular, assuming a hot gaseous mixture, CALPUFF
182 reproduces the plume up to its maximum height, corresponding to a null vertical velocity.
183 At this altitude continuous material emission is discretized in several packets (the *puffs*),
184 so that at each time-step a finite number of puffs are released. The mass flow rate
185 associated with the puffs matches the mass flow rate computed at the top of the rising
186 plume. Each puff is associated with a given particle size and release time. The number of

187 puffs is mainly determined by the wind speed at the source and is computed to adequately
188 represent a continuous release. The wind present at the altitude at which the puffs are
189 injected causes the puff center to move in the horizontal direction, whereas the settling
190 velocity, also acting on the puff center, brings the puffs towards the ground. During the
191 displacement the material inside the puff is affected by vertical and horizontal diffusion,
192 which causes the puff to spread. Under the assumption of Gaussian packets, their diffusion
193 is described by lateral and vertical standard deviations. Finally, it is worth noting that the
194 CALPUFF System has been validated through extensive comparison of model predictions
195 with experimental data such as the Cross-Appalachian Tracer Experiment (CAPTEX).
196 The CAPTEX experiment involved the release of a unique series of tracers for the purpose
197 of providing data to evaluate and improve computer models of pollutant dispersion and to
198 provide insight into the mechanisms of long-range transport and dispersion. To compare
199 CALPUFF to other widely used codes, further studies (Kincaid and Lovett data set) were
200 conducted; these studies suggest that the CALPUFF dispersion model allows appropriate
201 characterization of both local-scale and long-range transport and dispersion (*EPA U.S.*
202 [1998d]; *Earth Tech, Inc.* [2002]). Due to the model performance, the U.S. Environmental
203 Protection Agency (*EPA U.S.* [1998a]; *EPA U.S.* [1998b]; *EPA U.S.* [1998c]; *Irwin* [1998];
204 *Scire et al.* [2000]) proposed CALPUFF as a guideline model for regulatory applications
205 involving long-range transport and near-field applications where non-steady-state effects
206 may be important.

4. The VOL-CALPUFF Code

207 Fig. 2 illustrates the main features of the VOL-CALPUFF code we developed in the
208 present work. In the following sub-sections, the main equations and features of the new

209 model will be described by highlighting the main developments carried out with respect
210 to the original CALPUFF code.

4.1. Meteorological Pre-processors

211 The need to describe dispersal under the forcing of realistic meteorological conditions
212 makes the treatment of the original weather forecasting data a crucial step. The flow-
213 chart reported in Fig. 1 shows the presence of two different meteorological pre-processors
214 needed to provide VOL-CALPUFF with the required meteorological information. The
215 first, CALITA, is aimed at decoding and rewriting, in a format readable by CALMET,
216 the data produced in grib (GRIdded Binary, see *Stackpole* [1994]) format by the mesoscale
217 prognostic code. CALITA is optimized for working on meteorological data coming from
218 different sources as those produced by the Italian Lokal Modell (COSMO's web-site
219 [2004]). CALITA can also use meteorological data coming from the Reanalysis Archive of
220 the European Center for Medium-Range Weather Forecast (ECMWF) and National Cen-
221 ters for Environmental Prediction (NCEP-NOAA) in such a way that they can be read
222 by CALMET. Using CALITA it is possible to define the subdomain being investigated
223 and the number of atmospheric levels the user is interested in. It provides CALMET with
224 3D fields of pressure (and related geopotential height), temperature, wind direction, wind
225 speed, pressure vertical velocity and relative humidity, together with 2D field of pressure at
226 sea level, total rainfall accumulation and snow cover indicator. The second pre-processor,
227 CALMET, is a diagnostic model able to produce a quite simplified analysis of the at-
228 mosphere by describing either mesoscale dynamics or micrometeorological processes. The
229 latter includes an energy budget model for the computation of appropriate boundary layer
230 scaling parameters such as surface heat flux, surface momentum flux and boundary layer

231 height, which are used to derive the friction velocity, the convective velocity scale and the
232 Monin-Obukhov length (*Scire et al.* [1990]). In this study, we run CALMET in a “non-
233 observational” mode, i.e. without including assimilation of meteorological data coming
234 from weather stations, using mesoscale output files as an initial guess field. The spatial
235 resolution adopted is 1 km and applies to the entire computational domain.

4.2. Rising Plume Phase

236 This part of the VOL-CALPUFF code is new since the built-in plume rise model al-
237 ready implemented in CALPUFF was able to treat only gaseous emissions with a density
238 lower than atmospheric. Therefore a more general plume rise model was implemented in
239 VOL-CALPUFF to take into account the presence of a number of solid particulate phases.
240 The equation set was solved in a 2D Cartesian coordinate system (s, φ) by considering
241 the bulk properties of the eruptive mixture (see Fig. 2). The plume is assumed with
242 a circular section along the curvilinear coordinate s and an inclination on the ground
243 defined by an angle φ between the axial direction and the horizon. This last feature is
244 needed to describe the evolution of weak explosive eruptions which are strongly affected
245 by atmospheric conditions.

246 As in the plume theory, the entrainment (due to both turbulence in the rising buoyant
247 jet and to the crosswind field) is parameterized through the use of two entrainment co-
248 efficients, α and γ . The theory assumes that the efficiency of mixing with ambient air is
249 proportional to the product of a reference velocity (the vertical plume velocity in one case
250 and the wind field component along the plume centerline in the other), α and γ (*Morton*
251 [1959]; *Briggs* [1975]; *Wright* [1984]; *Weil* [1988]). Although this simplified approach can
252 be used to reproduce the first-order features of plume ascent (e.g. final plume height), it

253 does not explicitly describe more complex observed dynamics such as the double-vortex
 254 structure (*Ernst et al.* [1994]). The equation set consists of the equations of conservation
 255 of mass, momentum and thermal energy for the bulk mixture with height, equations ex-
 256 pressing the conservation of mass for pyroclasts of different sizes, and those describing the
 257 variation of specific heat and mixture gas constant. The equation system is completed
 258 by the perfect gas law for the gaseous phase by assuming equilibrium pressure conditions
 259 between the volcanic plume and surrounding atmosphere. The total mass conservation
 260 equation solved by the model is:

$$\begin{aligned}
 261 \quad \frac{d(\beta U_{sc} r^2)}{ds} &= 2r\rho_a[\alpha|U_{sc} - U_a \cos\varphi| + \gamma|U_a \sin\varphi|] + \\
 262 \quad &\quad -p\beta r(1-n) \sum_{i=1}^N w_s(i)y_i
 \end{aligned} \tag{1}$$

263 The variation of mass flux (l.h.s. term) is due to air entrainment and loss of solid
 264 particles (first and second r.h.s. terms, respectively). In Eq. (1), U_{sc} represents the
 265 velocity of the plume cross-section along its centerline, r the plume radius, β the mixture
 266 bulk density and U_a is the horizontal wind speed. This equation is similar to that used
 267 by *Bursik* [2001], the only difference being the lack of the re-entrainment term, which
 268 we assume to be negligible for the low intensity bent-over plumes discussed below and in
 269 the companion paper (*Ernst et al.* [1996]; *Bursik* [2001]). The factor p reflects, from a
 270 geometrical point of view, the possibility of each particle falling out from the rising plume
 271 and, by assuming clasts are lost only from the sloping plume margins, it is a function of
 272 the radial entrainment coefficient only (*Bursik et al.* [1992a]):

$$274 \quad p = \frac{2((1 + \frac{6}{5}\alpha)^2 - 1)}{(1 + \frac{6}{5}\alpha)^2 + 1} \tag{2}$$

For our values of α , the p factor varies between 0.2 and 0.33 ($\alpha=0.09$ and $\alpha=0.15$, respectively). The influence of the two entrainment coefficients, α and γ , was investigated through sensitivity studies (see next section), but in most cases they were set to 0.09 and 0.6, respectively, as determined in experimental studies by *Morton et al.* [1956], *Briggs* [1975] and *Weil* [1988]. As shown in the companion paper (*Barsotti and Neri* [2007], this issue), these values for the two coefficients can provide quite consistent estimates of plume height and deposit accumulation for the 2001 Etna plume investigated. In Eq. (1), the quantities $w_s(i)$ and y_i are the settling velocity and mass fraction, respectively, of the i -th granulometric class. The term in which they appear is the contribution of particle sedimentation from the plume.

Defining n as the mass fraction of the gaseous phase, the term $\pi\beta U_{sc}r^2(1-n)y_i$ represents the mass flux in the plume of the i -th particulate class. To compute the variation of the mass flux of solids during ascent the model solves the N mass conservation equations for the N particulate phases; which result in:

$$\frac{d(\beta U_{sc}r^2(1-n)y_i)}{ds} = -pw_s(i)\beta r(1-n)y_i \quad i = 1, \dots, N. \quad (3)$$

The X - and Z -components of the momentum balance solved by the model are:

$$\frac{d(\beta U_{sc}r^2(u - U_a))}{ds} = -r^2\beta w \frac{dU_a}{dz} - up\beta r(1-n) \sum_{i=1}^N w_s(i)y_i \quad (4)$$

$$\frac{d(\beta U_{sc}r^2w)}{ds} = gr^2(\rho_a - \beta) - wp\beta r(1-n) \sum_{i=1}^N w_s(i)y_i \quad (5)$$

where the two components of plume velocity along the X and Z axes are u and w , respectively, and are linked by the relation $U_{sc} = \sqrt{u^2 + w^2}$. In the r.h.s. of Eq. (4) appear the terms related to the exchange of momentum due to the wind and to momentum loss from the fall of solid particles. Similar contributions are evident in the r.h.s. term of Eq.

298 (5) where the vertical momentum is changed by the gravitational acceleration term and
 299 the segregation of particles.

300 Finally, following the above adopted notation, the equation for conservation of thermal
 301 energy solved by VOL-CALPUFF is described as:

$$\begin{aligned}
 302 \frac{d(\beta U_{sc} r^2 C_{pmix} T_p)}{ds} &= 2r\rho_a C_a T_a (\alpha |U_{sc} - U_a \cos\varphi + \gamma |U_a \sin\varphi|) + \\
 303 &\quad -r^2 w \rho_a g + \\
 304 &\quad -T_p p \beta r (1-n) * \sum_{i=1}^N C_s(i) w_s(i) y_i \tag{6}
 \end{aligned}$$

305 The first term on r.h.s. describes the cooling of the plume due to ambient air entrain-
 306 ment, the second one takes into account atmospheric thermal stratification, and the third
 307 term allows for heat loss due to sedimentation of solid particles. A thermal equilibrium
 308 between solid and gaseous phases is assumed. This formulation is similar to that proposed
 309 by *Glaze and Baloga* [1996] adapted for a two-dimensional and multi-phase treatment.

310 Finally, two equations for the variation rate of mixture specific heat and for the mixture
 311 gas constant were derived. Both variables were defined as weighted averages on the mass
 312 fraction of the components. We report the expression for the gas constant only, obtained
 313 knowing that the variation of gaseous mass fraction with height is solely due to entrained
 314 air:

$$315 \frac{dR_g}{ds} = \frac{n_0 \beta_0 U_{sc0} r_0^2 (R_{air} - R_{gv})}{n^2 \beta^2 U_{sc}^2 r^3} * 2\rho_a [\alpha |U_{sc} - U_a \cos\varphi| + \gamma |U_a \sin\varphi|] \tag{7}$$

317 where R_{gv} is the gas constant for the specific volcanic gas component. This formulation
 318 reduces, for particular cases, to the expressions of *Woods* [1988] and *Glaze and Baloga*
 319 [1996]. The plume rise equations were solved with a predictor-corrector Heun's scheme

320 that guarantees a second-order accuracy, keeping the execution time in the order of sec-
 321 onds. Vent boundary conditions include the initial plume radius (r_0), mixture velocity
 322 (U_{sc0}) and temperature (T_0), gas mass fraction (n_0) and the physical properties of the
 323 granulometric population.

4.3. Puff Transport and Diffusion

324 The mass flow rate feeding the puffs corresponds to the particle flow rate feeding the
 325 plume at the vent corrected for the amount radially lost during ascent. VOL-CALPUFF
 326 then describes pyroclast transport and diffusion in the atmosphere by tracking the move-
 327 ments of a number of Gaussian puffs, calculating their position, their lateral and vertical
 328 diffusion, and their amount of mass. Puff center displacement is computed by the simple
 329 relation $\bar{S} = \bar{V} * t$. Horizontally, the puff center is subjected to vertically-averaged zonal
 330 and meridional winds ($\bar{V}_H = \sqrt{U_{ave}^2 + V_{ave}^2}$), whereas vertically it is subjected only to the
 331 fall velocity ($\bar{V}_V = V_{set}$). The vertical component of the wind field is indirectly accounted
 332 for through a vertical spreading of the puff obtained by varying the vertical dispersion
 333 coefficient as a function of the vertical velocity gradient (*Scire et al.* [2000]). During puff
 334 movement, the mass distribution of a given particle size within the puff changes due to
 335 turbulent phenomena. Puff concentration is described by a Gaussian distribution whose
 336 standard deviations, horizontal and vertical, are computed for each time step. For a
 337 circular puff, the mathematical expression of such a distribution, which also represents
 338 the puff contribution to the concentration computed at a given location (*receptor*), is the
 339 following:

340

$$C(s) = \frac{Q(s)}{2\pi\sigma_y^2} g_t e^{-\frac{R^2(s)}{(2\sigma_y^2)}} \quad (8)$$

342

$$g_t = \frac{1}{(2\pi)^{\frac{1}{2}}\sigma_z} \sum_{n=-\infty}^{\infty} \left[e^{-\frac{(z_r - H_e + 2nh)^2}{(2\sigma_z^2)}} + e^{-\frac{(z_r + H_e + 2nh)^2}{(2\sigma_z^2)}} \right] \quad (9)$$

344 where s is the distance traveled by the puff from the source, $R(s)$ is the horizontal
 345 distance between puff center and receptor, and g_t is the vertical term, also called the
 346 coupling term, which depends on the puff and receptor relative positions. In particular,
 347 in case of puffs below the atmospheric boundary layer the coupling term takes into account,
 348 through the infinite sum over the index n , the material entrapment between the ground
 349 and the mixing lid of thickness h . Puff mass is represented by the variable Q and it varies
 350 with time by material removal due to sedimentation. Finally, the sigmas represent the
 351 horizontal and vertical diffusions. Their formulation is expressed as follows:

352

$$\sigma_{y,n}^2 = \sigma_{yt}^2 + \sigma_{ys}^2 + \sigma_{yb}^2 \quad (10)$$

353

354

$$\sigma_{z,n}^2 = \sigma_{zt}^2 + \sigma_{zb}^2 \quad (11)$$

355

356 where the horizontal term (Eq. (10)) contains the contribution due to atmospheric
 357 turbulence (σ_{yt}), the contribution due to a lateral (cross-wind) scale of the vent area-
 358 source (σ_{ys}) and the contribution due to plume buoyancy at the time of release (σ_{yb}).
 359 A similar formulation is valid for the vertical term (Eq. (11)), where the contribution
 360 due to areal extension is missing. These expressions show how the model allows the
 361 puffs to spread not only in response to atmospheric turbulence (σ_{yt} and σ_{zt}), but also in
 362 relation to the dynamics of the plume and to its structure when reaching the maximum

363 rise height. In particular, the puffs are characterized by lateral dispersal coefficients
364 (σ_{yb} and σ_{zb}) which are a function of the plume top radius. Furthermore the sigmas
365 ($\sigma_{y,n}$ and $\sigma_{z,n}$) are functions of travel time (from source to receptor) and are computed
366 each time the puff has a non-null contribution to the receptor. Finally, it should be
367 noted that, in contrast to CALPUFF, the VOL-CALPUFF code is able not only to track
368 the transport of puffs well above the atmospheric boundary layer (which can vary from
369 hundreds of meters to a few kilometers above the ground), but also to compute their
370 concentrations at the receptor locations. This extension of the code is indeed necessary
371 due both to the much greater heights reached by volcanic plumes with respect to emission
372 from industrial stacks and to our interest in mapping ash concentration anywhere, i.e. not
373 only on the ground. Additional features implemented in VOL-CALPUFF are related to
374 the consideration of particles with different diameters (up to several millimeters) and to
375 the effect of particle shape on their settling velocity. With respect to the first aspect, VOL-
376 CALPUFF can represent the multisize nature of the eruptive mixture by considering, at
377 each time step, different independent puffs, each one characterized by a specific particle
378 diameter. This is possible due to the dilute nature of the dispersal system that makes
379 the interaction between particles negligible (*Crowe et al.* [1998]). Regarding the second
380 aspect, several past and recent studies have highlighted the importance of describing
381 the effect of particle sizes (*Bonadonna et al.* [1998]) as well as non-sphericity on their
382 falling velocities (*Walker* [1971]; *Wilson* [1972]; *Wilson and Huang* [1979]; *Riley et al.*
383 [2003]; *Dellino et al.* [2005]). The original CALPUFF code restricts the computation of
384 settling velocity to the atmospheric layer affected by default activities and, as default,
385 uses Stokes's formulation for spherical particles. VOL-CALPUFF adopts a formulation of

386 the settling velocity as function of the Reynolds number. In particular, it adopts Stoke's
 387 drag coefficient expression $C_D=24/Rey$ for Reynolds numbers smaller than $Rey < 0.1$ and
 388 $C_D \sim 1$ for $Rey > 1000$ (*Walker* [1971]). For Reynolds numbers in the 0.1-100 range, the
 389 Wilson and Huang formulation is used (*Wilson and Huang* [1979]). The latter formulation
 390 appears to be a good trade-off between ease of formulation and accuracy of results. It
 391 defines the following relationship between the drag coefficient, C_D , and Reynolds number
 392 :

$$394 \quad C_D = \frac{24}{Rey} F^{-0.28} + 2\sqrt{1.07 - F} \quad (12)$$

395 in which particle shape affects the factor F through the equation $F = \frac{b+c}{2a}$, where
 396 a, b , and c are the three principal axes of the particle. Lastly, for intermediate values
 397 $100 < Rey < 1000$ a linear interpolation between the above described correlations is
 398 assumed for C_D (as already suggested by *Pfeiffer et al.* [2005]). The settling velocity of
 399 non-spherical particles is also allowed to vary as a function of height above the ground due
 400 to major variations in air density and viscosity with altitude (*Wilson* [1972]). In contrast,
 401 particle aggregation processes are not described by the present model, although they can
 402 play a major role in some conditions (*Textor and Ernst* [2004]; *Veitch and Woods* [2004]).

5. Initial Analyzes and Model Outputs

403 In this section first applications of the VOL-CALPUFF will be presented to show some
 404 of its standard outputs and type of results it is able to provide. In particular, the plume
 405 model was applied to the investigation of some interactions between plume rise and disper-
 406 sal processes and the atmospheric environment, in the case of weak explosive events. Mete-

407 orological data used were produced by the non-hydrostatic EURO-LM Model (COSMO's
408 web-site [2004]).

409 **Plume dynamics** Several simulations were performed by varying the conditions of the
410 eruptive mixture at the vent in a still vs. windy environment. The results obtained were
411 plotted in terms of variations of column density, velocity, and temperature with height
412 and also compared to previous models (*Woods* [1988]; *Bursik and Woods* [1991]; *Bursik*
413 [2001]). As an example, keeping constant the meteorological data and the vent velocity,
414 and increasing vent radius, the model reproduced the shift in eruptive style from buoyant
415 to super-buoyant and then to collapsing plumes, already predicted for plumes rising in a
416 still atmosphere (*Bursik and Woods* [1991]). But the novel feature of VOL-CALPUFF is
417 its ability to describe the effect of horizontal wind field on column evolution. As illustrated
418 in the companion paper (*Barsotti and Neri* [2007], this issue), this is an important new
419 feature of the code that strongly affects dispersal and deposition processes. This effect
420 is shown in Fig. 3 where the column height evolution with time is reported for a still
421 (thin line) and windy environment (bold one), for two intensities and for two seasonal
422 periods. Even for constant vent feeding, weather conditions can modify column height by
423 up to 100% or more. The sensitivity of plume dynamics to wind action is shown for an
424 intensity range typical of weak explosive eruptions. In the absence of wind, the influence
425 of atmospheric stratification on column height can also be inferred by comparing the tem-
426 poral column evolutions in different seasonal periods (summer vs. winter). During colder
427 periods, for both intensities, the plume reaches slightly greater heights in the atmosphere
428 (*Wilson and Walker* [1987]).

429 The effect of the wind field on plume tilting can be seen in Fig. 4. The figure reports

two different wind speed profiles (bold lines) and the associated distances reached by the
column axis along the vertical and downwind directions. In particular, Fig. 4a shows the
plume response to the tilting effect of wind for two real meteorological conditions, in the
early morning and at midday, for a mass flow rate of $6.6 * 10^3$ kg/s. Similarly, Fig. 4b
shows the results for a higher plume intensity ($2.5 * 10^4$ kg/s). The investigated wind
profiles produce quite different plume rise trajectories. From the figure it is evident how
the plume, meeting the more intense wind, rises about 25 % less high than that affected
by the weaker winds; whereas the downwind distance of the plume top is only slightly
sensitive.

VOL-CALPUFF can also be used to assess the sensitivity of results to the model pa-
rameters, for instance to the entrainment coefficients. Fig. 5a and Fig. 5b show the
variation of column height, calculated each hour during a 72-hour run with constant vent
conditions, as a function of the two entrainment coefficients. The figure clearly shows the
irregular trends which reflect the temporal variability of meteorological conditions met by
the column during ascent. However, the role of the entrainment coefficients (Eq. 1) in the
determination of column height is also evident. Keeping the wind-entrainment coefficient
 γ equal to 0.6, the radial-entrainment coefficient α was varied in the range 0.09-0.15 (Fig.
5a). The first value was proposed by *Morton et al.* [1956] and is typically assumed for
buoyant volcanic plumes (*Sparks et al.* [1997]). The second value comes from laboratory
experiments (*Hewett et al.* [1971]). In agreement with *Morton et al.* [1956] and *Wilson
and Walker* [1987], increasing the radial coefficient, α , the column reaches decreasing al-
titudes. The VOL-CALPUFF results show that, in a windy environment, this variation
is reflected in an approximately 30% change of column height.

453 A similar sensitivity study was performed for a variation of γ in the range 0.6-1.0 (derived
454 by *Briggs* [1975] and *Hewett et al.* [1971], respectively), confirming the inverse relation be-
455 tween column height and entrainment coefficient. The two simulations, keeping α equal
456 to 0.09, show a stronger dependence on wind-entrainment variation, which produces a
457 difference of up to about 40% in column height (Fig. 5b).

458 **Ash dispersal** In addition to the analysis of plume evolution, VOL-CALPUFF provides
459 consistent estimates of atmospheric ash concentrations and particle deposition at the
460 ground. Each hour it computes the quantity of emitted material still airborne and the
461 amount deposited. In our standard applications the domain is sliced into eight terrain-
462 following levels at 800 m intervals with each one made up of 5625 points. Both the
463 number of levels as well as the gridded points can be increased. Particle concentration
464 is computed at each receptor. Fig. 6 shows a vertical section of the domain used in the
465 application at Mt. Etna (discussed in the companion paper), in which levels have been
466 remapped referring to sea level. The horizontal levels are parallel planes in which the color
467 is graduated depending on the amount of computed ash. More intuitive is a planar view
468 representation where the contouring of particle concentration (g/m^3), at a specific altitude
469 above the ground, is superimposed on a 2D topography (Fig. 7). The code's Lagrangian
470 nature and the algorithms's structure make it easy to quantify the presence of ash in
471 specific locations and at any height of interest, for example in correspondence of airplane
472 flight levels or corresponding to areas with anthropogenic activities. Ash concentration
473 estimates at plume levels may prove valuable to fine tune remote-sensing instruments as
474 regards particle diameter and density, as well as, detection thresholds. Finally, at the
475 ground level, VOL-CALPUFF can compute the dry-fluxes of depositing material from

476 which the ash load is estimated in kg/m^2 . A 3D representation of this output is provided
477 by Fig. 8, in which the computed deposit is *spread* on a 3D orographic profile.

6. Conclusive Remarks

478 The VOL-CALPUFF model is a new quantitative tool for simulating atmospheric dis-
479 persal and deposition of volcanic ashes. The main new feature of the model is its ability to
480 combine plume rise and ash dispersal models to describe their dynamics under the action
481 of realistic 3D and time-dependent meteorological conditions. The model, by adopting a
482 mixed Eulerian-Lagrangian formulation, is able to describe effectively the rising column
483 and regional ash dispersal throughout the eruption. The Lagrangian description of ash
484 dispersal provides a reliable model both in the distal and proximal areas. Moreover, spa-
485 tial and temporal resolution scales in the order of 1 km and 1 hour, respectively, can be
486 provided by VOL-CALPUFF by keeping the computational time to a few minutes even
487 for eruptive events lasting several days. This feature makes VOL-CALPUFF a promising
488 tool also for the production of quasi real-time ash dispersal forecast simulations to be used
489 for warning and hazard analysis (*Barsotti et al.* [2006]). Results from initial simulations
490 clearly highlight the novel features of the model and the important implications that they
491 allow regarding dispersal dynamics. With specific reference to the rising plume dynamics,
492 the results presented show the extensive influence of meteorological conditions on plume
493 height. The wind speed variations during the three-day period investigated result in the
494 plume height variations of well above 100%. An increase in wind speed by a few meters
495 per second at low altitude can significantly tilt the rising plume, shifting the plume top
496 several hundreds of meters closer to the ground (see Fig. 4). In absence of wind, the col-
497 umn height also shows sensitivity to the variations of atmospheric thermal stratification.

498 In the companion paper (*Barsotti and Neri* [2007], this issue) VOL-CALPUFF is used to
499 model a weak plume from Mt. Etna, and results are compared to independent observa-
500 tions to better describe VOL-CALPUFF capabilities and limitations. Model applications
501 to larger plumes are being prepared and will be presented in future works.

502 **Acknowledgments.**

503 This work was supported by the European Union (project EXPLORIS, contract
504 no.EVR1-CT-2002-40026), Dipartimento di Protezione Civile (Italy) (project V3-6
505 Etna) and Ministero Dell'Istruzione, Università e Ricerca (Italy) (project FIRB no.
506 RBAP04EF3A_005). The staff of Earth Tech Inc. (now TRC Companies, Inc.) (US)
507 is warmly acknowledged for its support and help during the stay of SB at Concord, US.
508 Gerald Ernst and Greg Valentine provided very useful reviews of the manuscript.

Notation

a	major mean particle axes
b	median mean particle axes
c	minor mean particle axes
C_{pmix}	heat capacity of mixture
C_a	heat capacity of ambient air
C_D	drag coefficient
C_s	heat capacity of solid phase
$C(s)$	concentration at receptor
F	particle shape factor
g_t	coupling vertical term
H_e	effective puff height
h	mixing layer height
n	gas mass fraction
n_0	initial gas mass fraction
p	probability of fallout
$Q(s)$	amount of material in each puff
r	plume radius
r_0	initial plume radius
R_{gv}	gas constant for volcanic gas component
R_g	gas constant for mixture gas phase
R_{air}	gas constant of ambient air
Rey	Reynolds's number
s	downstream coordinate or source-puff distance
\bar{S}	generic puff displacement
t	time
T_a	ambient temperature
T_p	plume temperature
T_0	initial mixture temperature
U_{ave}	zonal wind averaged over lateral puff extension
U_{sc}	centerline plume velocity
U_{sc0}	initial centerline plume velocity
U_a	wind speed
V_{ave}	meridional wind averaged over lateral puff extension
V_{set}	settling velocity
\bar{V}	generic velocity (both horizontal and vertical) driving puff displacement
\bar{V}_H	horizontal puff velocity
\bar{V}_V	vertical puff velocity
$w_s(i)$	settling velocity of i-th granulometric class
y_i	mass fraction of i-th granulometric class
z_r	receptor height

Notation

α	radial entrainment coefficient
β	mixture bulk density
β_0	initial mixture bulk density
γ	wind-entrainment coefficient
φ	angle between plume axis and horizon
ρ_a	air ambient density
$\sigma_{y,n}$	lateral dispersion coefficient at n time step
σ_{yb}	lateral dispersion coefficient due to plume buoyancy
σ_{ys}	lateral dispersion coefficient due to lateral scale of an area-source
σ_{yt}	lateral dispersion coefficient due to atmospheric turbulence
$\sigma_{z,n}$	vertical dispersion coefficient at n time step
σ_{zb}	vertical dispersion coefficient due to plume buoyancy
σ_{zt}	vertical dispersion coefficient due to atmospheric turbulence

References

- 509 Armienti, P., G. Macedonio, and M.T. Pareschi (1988), A numerical-model for simulation
510 of tephra transport and deposition - applications to May 18, 1980, Mount-St-Helens
511 eruption, *J. Geophys. Res.*, *93*, 6463–6476.
- 512 Barsotti, S. and A. Neri (2007), The VOL-CALPUFF model for atmospheric ash dispersal:
513 II. Application to the Weak Mt. Etna Plume of July 2001, submitted to *J. Geophys.*
514 *Res.*.
- 515 Barsotti, S., L. Nannipieri and A. Neri (2006), An early-warning system for volcanic ash
516 dispersal: The MAFALDA procedure, Abstract no. V21C-06 AGU Fall Meeting, San
517 Francisco, CA, 11-15 December 2006.
- 518 Bonadonna, C., G. G. J. Ernst and R. S. J. Sparks (1998), Thickness variations and
519 volume estimates of tephra fall deposits: The importance of particle Reynolds number,
520 *J. Volcanol. Geotherm. Res.* *81*, 173-187.
- 521 Bonadonna, C., G. Macedonio and R. S. J. Sparks (2002), Numerical modelling of tephra
522 fallout associated with dome collapses and Vulcanian explosions: Application to haz-

523 ard assessment on Montserrat, in *The eruption of Soufriere Hills Volcano, Montserrat,*
524 *from 1995 to 1999, Geological Society Memoir*, no.21, edited by T.H. Druitt and B.P.
525 Kokelaar, pp. 517–537, Geological Society of London, Bath, UK.

526 Bonadonna, C., C. B. Connor, B. F. Houghton, L. Connor, M. Byrne, A. Laing and
527 T. K. Hincks (2005), Probabilistic modeling tephra dispersal: Hazard assessment to a
528 multiphase rhyolitic eruption at Tarawera, New Zealand, *J. Geophys. Res.*, *110*, B03203,
529 doi:10.1029/2003JB002896.

530 Briggs, G. A. (1975), Plume rise predictions, in *Lectures on air pollution and environmen-*
531 *tal impact analyses*, edited by Duane A. Hangen, pp. 59–111, American Meteorological
532 Society, Boston, MA.

533 Bursik, M. I. (2001), Effect of wind on the rise height of volcanic plumes, *Geophys. Res.*
534 *Lett.*, *28*, 3621–3624.

535 Bursik, M. I. and A. W. Woods (1991), Buoyant, superbuoyant and collapsing eruption
536 columns, *J. Volcanol. Geotherm. Res.*, *45*, 347–350.

537 Bursik, M. I., R. S. J. Sparks, S. N. Carey and J. S. Gilbert (1992a), Sedimentation of
538 tephra by volcanic plumes: I Theory and its comparison with a study of the Fogo A
539 plinian deposit, Sao Miguel (Azores), *Bull. Volcanol.*, *54*, 329–344.

540 Bursik, M. I., S. N. Carey and R. S. J. Sparks (1992b), A gravity current model for the
541 May 18, 1980 Mount St. Helens plume, *Geophys. Res. Lett.*, *19*, 1663–1666.

542 Carey, S. N. and R. S. J. Sparks (1986), Quantitative models of the fallout and dispersal
543 of tephra from volcanic eruption columns, *Bull. Volcanol.*, *48*, 109–125.

544 Costa, A., G. Macedonio and A. Folch (2006), A three-dimensional Eulerian model for
545 transport and deposition of volcanic ashes, *Earth and Science Planetary Letters*, *241*,

546 634–647.

547 Consortium for Small-scale Modeling (COSMO)’s web-site: <http://cosmo-model.cscs.ch/>

548 Crowe, C., M. Sommerfeld and Y. Tsuji (1998), Multiphase flows with droplets and par-
549 ticles, CRC Press, Boca Raton, Florida.

550 Dartevelle, S., W. I. Rose, J. Stix, K. Kelfoun and J. W. Vallance (2004), Numerical
551 modeling of geophysical granular flows: 2. Computer simulations of Plinian clouds
552 and pyroclastic flows and surges, *Geochemistry Geophysics Geosystem*, 5, Q08004, doi:
553 10.1029/2003GC000637.

554 Dellino, P., D. Mele, R. Bonasia, G. Braia, L. La Volpe and R. Sulpizio (2005), The
555 analysis of the influence of pumice shape on its terminal velocity, *Geophys. Res. Lett.*,
556 32, L21306, doi:10.1029/2005GL023954.

557 Draxler, R. R. and A. D. Taylor (1982), Horizontal dispersion parameters for long-range
558 transport modelling, *J. Appl. Met.*, 21, 367–372.

559 Draxler, R. R. and G. D. Hess (1998), An overview of the HYSPLIT_4 modelling system
560 for trajectories, dispersion and deposition, *Austral. Meteorol. Mag.*, 47, 295–308.

561 Earth Tech, Inc. (2002), Application of CALMET/CALPUFF and MESOPUFF II to
562 compare regulatory design concentrations for a typical long-range transport analysis,
563 U. S. EPA Report, Earth Tech, 196 Baker Avenue, Concord, Massachusetts 01742.

564 Environmental Protection Agency U.S. (1998a), A comparison of CALPUFF modelling
565 results to two tracer field experiment, EPA-454/R-98-009, Office of Air Quality Planning
566 and Standards, U. S. EPA, Research Triangle Park, NC 27711.

567 Environmental Protection Agency U.S. (1998b), An analysis of the CALMET/CALPUFF
568 modeling system in a screening mode, EPA-454/R-98-010, Office of Air Quality Planning

- 569 and Standards, U. S. EPA, Research Triangle Park, NC 27711.
- 570 Environmental Protection Agency U.S. (1998c), A comparison of CALMET/CALPUFF
571 with ISC3, EPA-454/R-98-020, Office of Air Quality Planning and Standards, U. S.
572 EPA, Research Triangle Park, NC 27711.
- 573 Environmental Protection Agency U.S. (1998d), Interagency Workgroup on air quality
574 modelling (IWAQM) Phase2: Summary report and recommendations for modelling
575 long range transport impacts, EPA-454/R-98-019, Office of Air Quality Planning and
576 Standards, U. S. EPA, Research Triangle Park, NC 27711.
- 577 Ernst, G. G. J., J. P. Davis and R. S. J. Sparks (1994), Bifurcation of volcanic plumes in
578 crosswind, *Bull. Volcanol.*, *56*, 159–169.
- 579 Ernst, G. G. J., R. S. J. Sparks, S. N. Carey and M.I. Bursik (1996), Sedimentation from
580 turbulent jets and plumes, *J. Geophys. Res.*, *101*, 5575–5589.
- 581 Glaze, L. S. and S. M. Baloga (1996), Sensitivity of buoyant plume heights to ambient
582 atmospheric conditions: Implications for volcanic eruption columns, *J. Geophys. Res.*,
583 *101*, 1529–1540.
- 584 Graf, H. F., M. Herzog, J. M. Oberhuber and C. Textor (1999), Effect of environmental
585 conditions on volcanic plume rise, *J. Geophys. Res.*, *104*, 24309–24320.
- 586 Heffter, J. L. and B. J. B. Stunder (1993), Volcanic ash forecasting transport and disper-
587 sion (VAFTAD) model, *Weath. Forecast.*, *8*, 533–541.
- 588 Herzog, M., H-F. Graf, C. Textor and J. M. Oberhuber (1998), The effect of phase changes
589 of water on the development of volcanic plumes, *J. Volcanol. Geotherm. Res.*, *87*, 55–74.
- 590 Hewett, T. A., J. A. Fay and D. P. Hoult (1971), Laboratory experiments of smokestack
591 plumes in a stable atmosphere, *Atmos. Environ.*, *5*, 769–789.

592 Houlst, D. P. and J. C. Weil (1972), A turbulent plume in laminar crossflow, *Atmos.*
593 *Environ.*, *6*, 513–531.

594 Irwin, J. S. (1998), Interagency Workgroup on Air Quality Modeling (IWAQM) Phase2:
595 Summary report and recommendations for modeling long range transport impacts, EPA-
596 454/R-98-019, Office of Air Quality Planning and Standards, U.S.EPA, Research Triangle
597 Park, NC.

598 Macedonio, G., M.T. Pareschi, and R. Santacroce (1988), A numerical simulation of the
599 Plinian fall phase of 79 AD eruption of Vesuvius, *J. Geophys. Res.*, *93*, 14817–14827.

600 Macedonio, G., M.T. Pareschi, and R. Santacroce (1990), Renewal of explosive activity
601 at Vesuvius: Models for the expected tephra fallout, *J. Volcanol. Geotherm. Res.*, *40*,
602 327–342.

603 Macedonio, G., A. Costa and A. Longo (2005), A computer model for volcanic ash fallout
604 and assessment of subsequent hazard, *Computer & Geosciences*, *31*, 837–845.

605 Martì, J. and G. G. J. Ernst (eds. 2005), *Volcanoes and the Environment*, Cambridge
606 University Press, Cambridge, UK.

607 Morton, B. R. (1959), Forced plumes, *J. Fluid Mech.*, *5*, 151–163.

608 Morton, B. R., F. R. S. Taylor and J. S. Turner (1956), Turbulent gravitational convection
609 from maintained and instantaneous sources, *Proceedings of the Royal Society of London*,
610 *234*, 1–23.

611 Nguyen, K. C., J. A. Noonan, I. E. Galbally and W. L. Physick (1997), Predictions
612 of plume dispersion in complex terrain: Eulerian versus Lagrangian models, *Atmos.*
613 *Environ.*, *31*, 947–958.

- 614 Oberhuber, J. M., M. Herzog, H. F. Graf and K. Schwanke (1998), Volcanic plume simu-
615 lation on large scales, *J. Volcanol. Geotherm. Res.*, *87*, 29–53.
- 616 Pfeiffer, T., A. Costa and G. Macedonio (2005), A model for the numerical simulation of
617 tephra fall deposits, *J. Volcanol. Geotherm. Res.*, *140*, 273–294.
- 618 Piedelievre, J. P., L. Musson-Genon and F. Bompay (1990), MEDIA - An Eulerian model
619 of atmospheric dispersion: a first validation on the Chernobyl release, *J. Appl. Meteor.*,
620 *29*, 1205–1220.
- 621 Riley, C. M., W. I. Rose and G. J. S. Bluth (2003), Quantitative shape measurements of
622 distal volcanic ash, *J. Geophys. Res.*, *108*, 2504, doi:10.1029/2001JB000818.
- 623 Scire, J. S., E. M. Insley and R. J. Yamartino (1990), Model formulation and user’s guide
624 for the CALMET meteorological model, Report, Sigma Research Corp., Concord, MA,
625 USA.
- 626 Scire, J. S. and F. R. Robe (1997), Fine scale application of the CALMET meteorological
627 model to a complex terrain site, Air&Waste Management Association’s 90th Annual
628 Meeting & Exhibition, Toronto, Ontario, Canada, June 8-13.
- 629 Scire, J. S., D. G. Strimaitis and R. J. Yamartino (2000), CALPUFF User’s guide, avail-
630 able at <http://www.src.com/calpuff/download/download.htm>
- 631 Searcy, C., K. Dean and W. Stringer (1998), PUFF: A Lagrangian trajectory volcanic ash
632 tracking model, *J. Volcanol. Geotherm. Res.*, *80*, 1–16.
- 633 Sigurdsson, H., B. Houghton, H. Rymer, J. Stix and S. McNutt (2000), *Encyclopedia of*
634 *volcanoes*, Academic Press, San Diego, CA.
- 635 Simpson, J. J., G. L. Hufford, R. Servranckx, J. S. Berg and C. Bauer (2002), The
636 February 2001 eruption of Mt. Cleveland, Alaska: Case study of an aviation hazard,

- 637 *American Meteor. Soc.*, 17, 691–704.
- 638 Sparks, R. S. J. (1986), The dimensions and dynamics of volcanic eruption columns, *Bull.*
639 *Volcanol.*, 41, 1–9.
- 640 Sparks, R. S. J., S. N. Carey and H. Sigurdsson (1991), Sedimentation from gravity
641 currents generated by turbulent plumes, *Sedimentology*, 38, 839–856.
- 642 Sparks, R. S. J., M. I. Bursik, S. N. Carey, J. S. Gilbert, L. S. Glaze, H. Sigurdsson and
643 A. W. Woods (1997), *Volcanic plumes*, J. Wiley, New York.
- 644 Stackpole, J. D. (1994), A guide to GRIB (Edition 1) The WMO format for the storage of
645 weather product information and the exchange of weather product messages in gridded
646 binary form, Automation Division, National Meteorological Center, National Weather
647 service, NOAA.
- 648 Suzuki, T. (1983), A theoretical model for dispersion tephra, in *Arc volcanism: Physics*
649 *and Tectonics*, edited by Shimozuru D. and I. Yokoyama, 93–113, Terra Scientific Pub-
650 lishing Company, Tokyo.
- 651 Suzuki, Y. J., T. Koyaguchi, M. Ogawa and I. Hachisu (2005), A numerical study of
652 turbulent behaviour in eruption clouds using a three dimensional fluid-dynamics model,
653 *J. Geophys. Res.*, 110, B08201, doi:10.1029/2004JB003460.
- 654 Textor, C. and G. G. J. Ernst (2004), Comment on "Particle aggregation in volcanic
655 eruption columns" by Graham Veitch and Andrew W. Woods, *J. Geophys. Res.*, 109
656 (B5), B05202, doi:10.1029/2002JB002291.
- 657 Textor, C., G. G. J. Ernst, M. Herzog and A. Tupper (2004), Potential of the ATHAM
658 model for Use in air traffic safety, Proceedings of 2nd International Conference on
659 Volcanic Ash and Aviation Safety, VAAS, pp. 15–19, OFCM, Alexandria, Virginia,

- 660 USA, June 21-24.
- 661 Textor, C., H. F. Graf, M. Herzog, J. M. Oberhuber, W. I. Rose and G. G. J. Ernst (2006a),
662 Volcanic particle aggregation in explosive eruption columns. Part I: Parameterization of
663 the microphysics of hydrometeors and ash, *J. Volcanol. Geotherm. Res.*, *150*, 359–377.
- 664 Textor, C., H. F. Graf, M. Herzog, J. M. Oberhuber, W. I. Rose and G. G. J. Ernst
665 (2006b), Volcanic particle aggregation in explosive eruption columns. Part II: Numerical
666 experiments, *J. Volcanol. Geotherm. Res.*, *150*, 378–394.
- 667 Veitch, G. and A. W. Woods (2002), Particle recycling in volcanic plumes, *Bull. Volcanol.*,
668 *64*, 31–39.
- 669 Veitch, G. and A. W. Woods (2004), Reply to comment by C. Textor and G. G. J. Ernst on
670 particle aggregation in volcanic eruption columns, *J. Geophys. Res.* *109*, (B5), B05203,
671 doi:10.1029/2003JB002388.
- 672 Walker, G. P. L. (1971), Grain-size characteristics of pyroclastic deposits, *J. Geol.*, *79*,
673 696–714.
- 674 Watkin, S., S. Karlsdóttir, N. Gait, D. Ryall and H. Watkin (2004), Volcanic ash monitor-
675 ing and forecasting at the London VAAC, Proceedings of 2nd International Conference
676 on Volcanic Ash and Aviation Safety, VAAS, pp. 65–69, OFCM, Alexandria, Virginia,
677 USA, June 21-24.
- 678 Weil, J. C. (1988), Plume rise, in *Lectures on air pollution modelling*, Editors Venkatram
679 A. and Wyngaard J. C., 119–166
- 680 Wilson, L. (1972), Explosive volcanic eruptions II. The atmospheric trajectories of pyro-
681 clast, *Geophys. J. R. astr. Soc.*, *30*, 381–392.

- 682 Wilson, L. (1976), Explosive volcanic eruptions III. Plinian eruption columns, *Geophys.*
683 *J. R. astr. Soc.*, *45*, 543–556.
- 684 Wilson, L. and T. C. Huang (1979), The influence of shape on the atmospheric settling
685 velocity of volcanic ash particles, *Earth and Planetary Science Letters*, *44*, 311–324.
- 686 Wilson, L. and G. P. Walker (1987), Explosive volcanic eruptions VI. Ejecta dispersal in
687 plinian eruptions: the control eruption conditions and atmospheric properties, *Geophys.*
688 *J. R. astr. Soc.*, *89*, 657–679.
- 689 Woods, A. W. (1988), The fluid dynamics and thermodynamics of eruption columns, *Bull.*
690 *Volcanol.*, *50*, 169–193.
- 691 Woods, A. W. and M. I. Bursik (1991), Particle fallout, thermal disequilibrium and vol-
692 canic plumes, *Bull. Volcanol.*, *53*, 559–570.
- 693 Wright, S. J. (1984), Buoyant jets in density-stratified crossflow, *J. Hydr. Eng.*, *110*, *5*,
694 643–656.

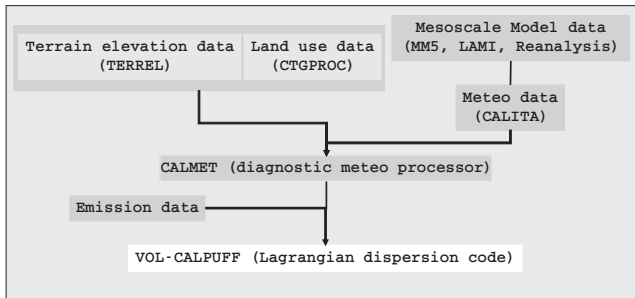


Figure 1. The simplified flowchart of CALPUFF as used in our application. It represents the minimal structure for running the system. It contains the meteorological and geophysical preprocessors (TERREL, CTGPROC, CALITA), the diagnostic meteorological model (CALMET), and the dispersal code (VOL-CALPUFF).

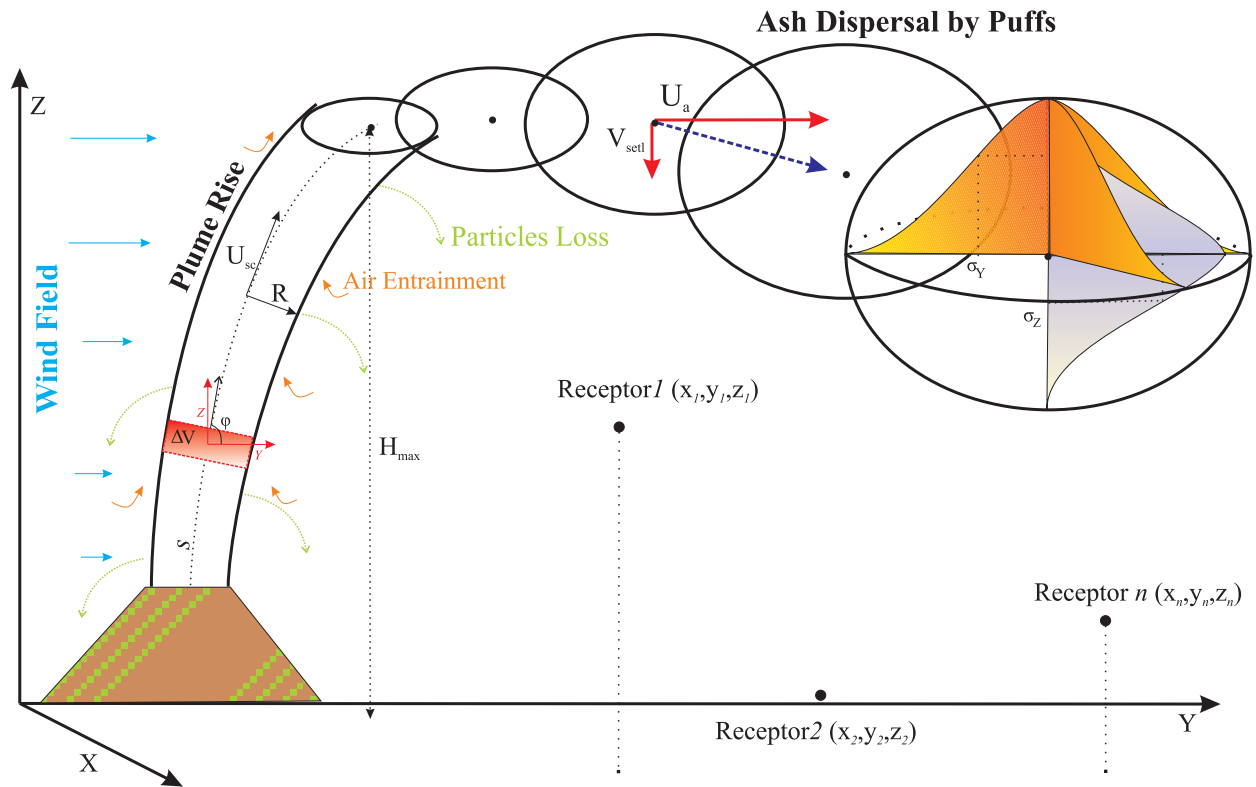


Figure 2. Schematic representation of the VOL-CALPUFF approach. Plume ascent is described by adopting a Eulerian formulation whereas dispersal is represented by a Lagrangian approach, i.e. following the movement and diffusion of a discrete number of puffs.

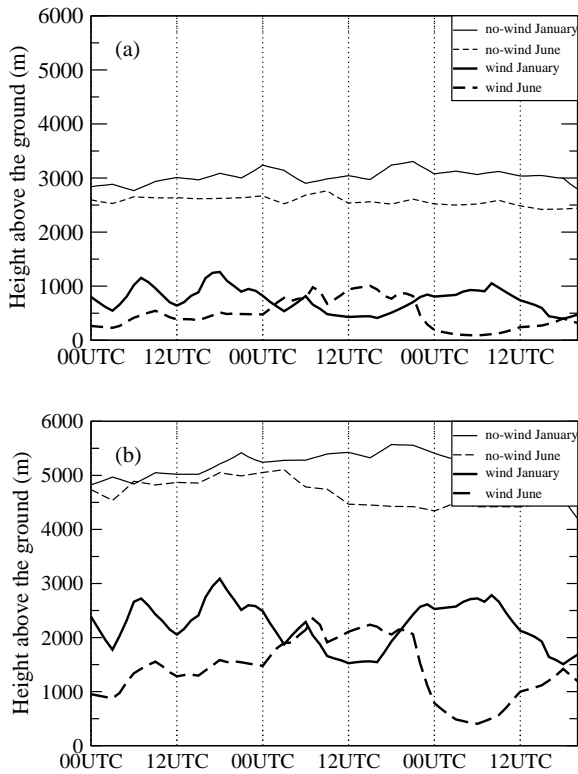


Figure 3. Variation of column height for two plume intensities, (a) $6.6 * 10^3$ kg/s ($T_0=1300$ K, $U_{sc0}=20$ m/s, $r_0=4.8$ m, $n_0=3\%$) and (b) $2.5 * 10^4$ kg/s ($T_0=1300$ K, $U_{sc0}=25$ m/s, $r_0=8.7$ m, $n_0=3\%$). Curves refer to a still (thin line) and windy (bold line) atmosphere, and to two different seasonal periods. In detail dashed lines refer to three days of June 2005 whereas the continuous ones indicate three days of January 2006.

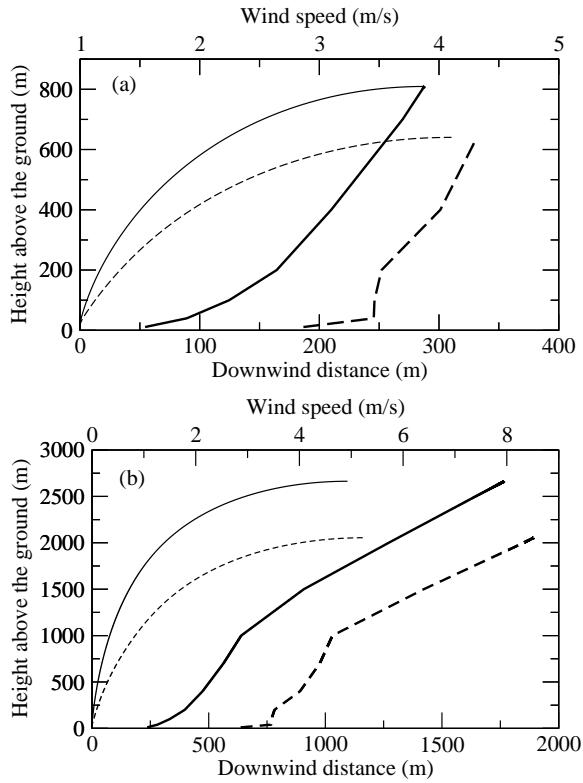


Figure 4. Effect of wind field on plume height and tilting for two different plume intensities and meteorological conditions. The intensities correspond to (a) 6.6×10^3 kg/s and (b) 2.5×10^4 kg/s and vent conditions are the same as Fig. 3. Wind profiles refer to 0600UTC and 1300UTC on 4 January 2006. From the figure it is clear how more intense speeds (dashed line) tilt the columns more than in the weaker cases (continuous line), reaching lower heights.

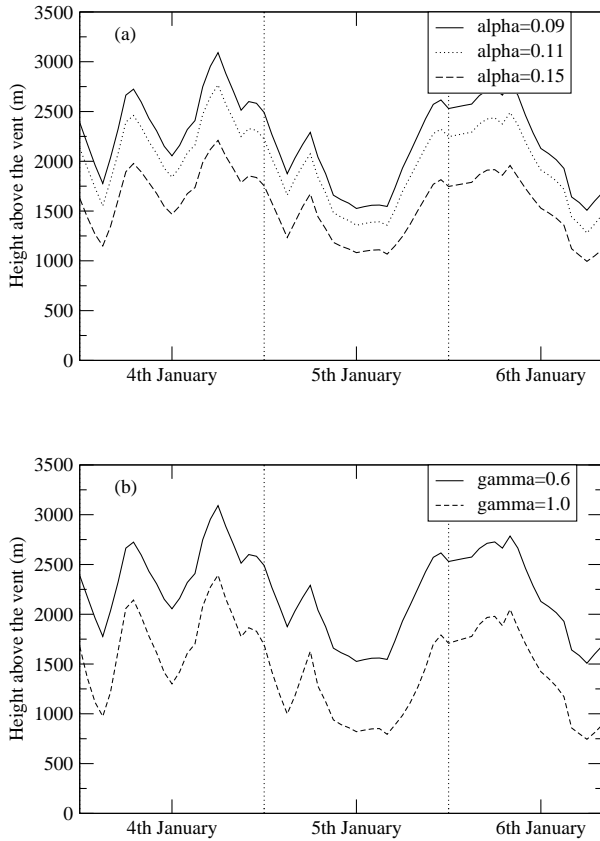


Figure 5. Temporal variations of column height for a mass-flow rate equal to 2.5×10^4 kg/s (the vent conditions are the same as Fig.3). The figures report the height trend over about three days (4-6 January 2006) under the forcing of realistic 3D meteorological conditions. The curves were obtained using different entrainment coefficient values. Keeping $\gamma=0.6$ three values of α are investigated (a): $\alpha = 0.11$ (dotted line), $\alpha = 0.15$ (dashed line) and $\alpha = 0.09$ (continuous line). And, keeping $\alpha=0.09$, two values of γ (b): $\gamma = 0.6$ (continuous line) and $\gamma=1.0$ (dashed line).

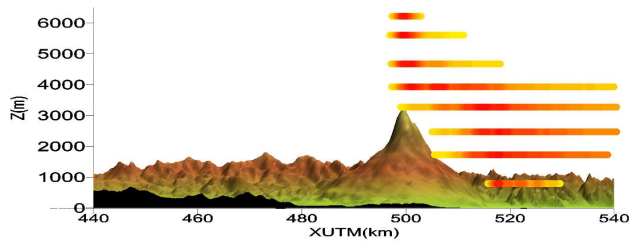


Figure 6. Vertical section of the 3D physical domain in which the horizontally extended levels, remapped from the standard terrain-following ones, are visible. In this case, VOL-CALPUFF adopted eight levels each one made up of 5625 nodes.

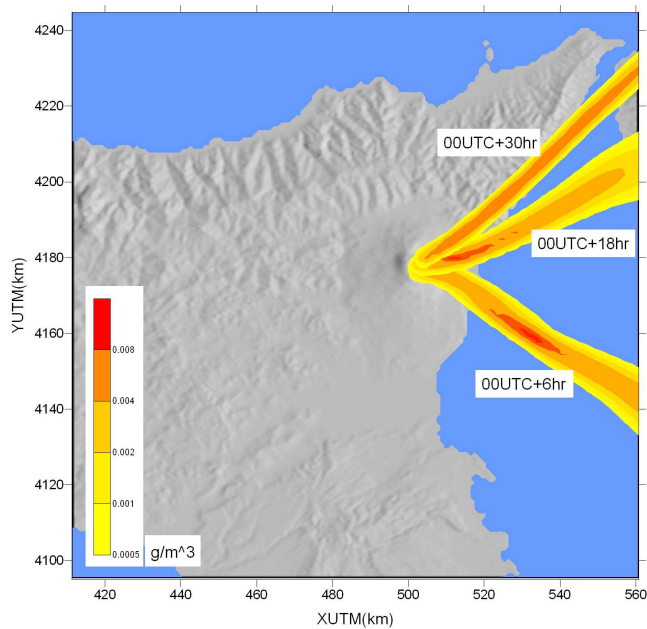


Figure 7. Contouring of $64\mu\text{m}$ particles concentration at 2400 m a.g.l. in a 2D representation of the VOL-CALPUFF outputs. The three snapshots correspond to three temporal instants at 12hr intervals. Variations in wind direction deflect the plume from SE to a NE dispersal.

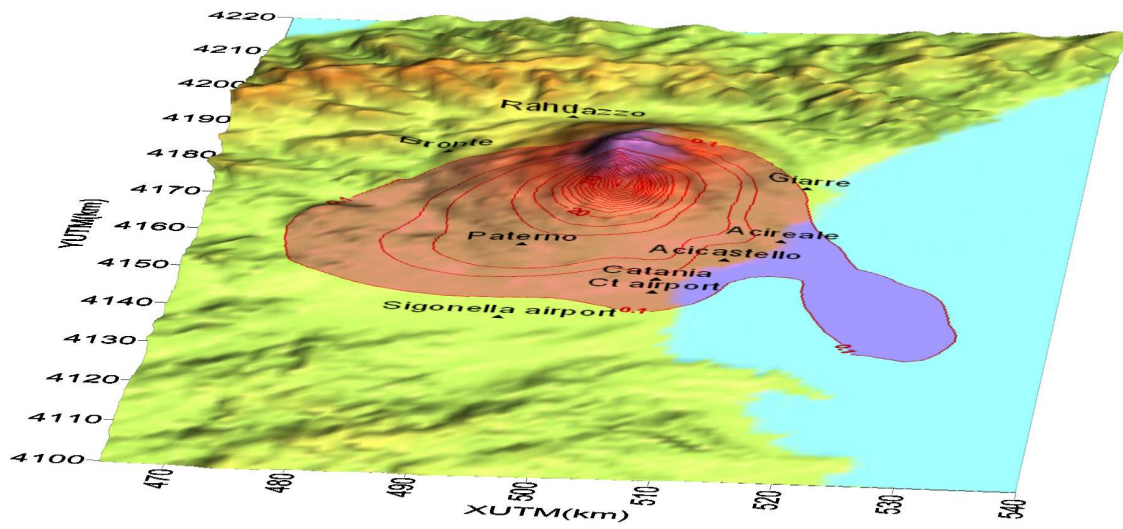


Figure 8. A given example of deposit on the ground at Mt.Etna. VOL-CALPUFF computes the deposited ash amount in kg/m^2 ; the lower reported value is equal to 0.1.